npj | parkinson's disease

Article

Published in partnership with the Parkinson's Foundation

https://doi.org/10.1038/s41531-025-01160-3

Modelling cholinergic and dopaminergic function over time in Parkinson's disease with and without *GBA1* variants

Check for updates

Sofie Slingerland[1,7] ✉, Eline K. R. de Meyer[2,3,7], Harm J. van der Horn[1], Giulia Carli[2,4], Anne C. Slomp[1,5], Emile d'Angremont[6], Jeffrey M. Boertien[1], Ingeborg Goethals[3], Sanne K. Meles[1,2], Sygrid van der Zee[1,5] & Teus van Laar[1]

Parkinson's Disease (PD) patients carrying *GBA1*-variants (GBA-PD) often show a faster cognitive decline, suggesting accelerated cholinergic degeneration. This study investigated changes over time in whole-brain cholinergic innervation within the context of dopaminergic changes and clinical outcomes in GBA-PD versus non-GBA-PD. 171 PD participants (44 GBA-PD, 127 non-GBA-PD) underwent clinical and neuropsychological assessments, brain MRI, ^{18}F-fluoroethoxy-benzovesamicol (^{18}F-FEOBV) PET (cholinergic) and 3,4-dihydroxy-6-^{18}F-fluoro-l-phenylalanine (^{18}F-FDOPA) PET (dopaminergic) imaging. GBA-PD participants showed worse executive functioning than non-GBA-PD. Voxel-wise linear mixed-effects models showed that GBA-PD exhibited lower ^{18}F-FEOBV binding in the right precentral and middle frontal gyrus, independent of age and sex, despite similar cholinergic decline over time. No *GBA1*-related differences were found in dopaminergic signal or its progression. Age and time since diagnosis were associated with progressive cholinergic and dopaminergic denervation in all patients. This first dual-tracer longitudinal PET study highlights early cholinergic involvement in GBA-PD and supports further evaluation of ^{18}F-FEOBV PET as biomarker.

Heterozygous variants in the *GBA1*-gene, which is responsible for encoding the lysosomal enzyme glucocerebrosidase, represent the most prevalent genetic risk factor for Parkinson's disease (PD)[1,2]. PD patients carrying *GBA1*-variants (GBA-PD) typically experience a more aggressive disease progression compared to those without such variants (non-GBA-PD) and suffer from worse motor impairment and more non-motor symptoms, including cognitive decline, neuropsychiatric symptoms and autonomic dysfunction[3–6].

Degeneration of the cholinergic system is related to cognitive decline in PD and dementia with Lewy bodies[7–9]. GBA-PD is characterized by a faster and more severe cognitive impairment compared to sporadic PD, suggesting a distinct role for the cholinergic system in *GBA1* variant carriers[10–12]. [^{18}F]Fluoroethoxybenzovesamicol (^{18}F-FEOBV) PET is a highly selective marker of in vivo cerebral cholinergic presynaptic terminal integrity, binding to the vesicular acetylcholine transporter[13–15]. In our previous cross-sectional study, we showed that in a cohort of de novo PD patients compared to controls, GBA-PD exhibited more extensive cholinergic degeneration in posterior regions compared to non-GBA-PD patients, despite having similar clinical characteristics at the time of diagnosis[16]. How these cholinergic changes progress over time between GBA and non-GBA PD is still unknown, which is one of the topics of this paper.

Moreover, cholinergic system changes should be examined within a broader pathophysiological context, particularly in relation to dopaminergic degeneration[12]. Although cholinergic degeneration plays a key role in cognitive decline, the more aggressive overall disease course in GBA-PD also raises the possibility of distinct dopaminergic involvement. However, previous neuroimaging studies reported inconsistent findings on dopaminergic differences between GBA-PD and non-GBA-PD, ranging from more

[1]Department of Neurology, University of Groningen, University Medical Center Groningen, Groningen, The Netherlands. [2]Department of Nuclear Medicine and Molecular Imaging, University of Groningen, University Medical Center Groningen, Groningen, The Netherlands. [3]Department of Diagnostic Sciences, University of Ghent, Gent, Belgium. [4]Department of Neurology, University of Michigan, Ann Arbor, MI, USA. [5]Department of Neurology, Division of Clinical Neuropsychology, University of Groningen, University Medical Center, Groningen, The Netherlands. [6]Department of Biomedical Sciences, University of Groningen, University Medical Center Groningen, Groningen, The Netherlands. [7]These authors contributed equally: Sofie Slingerland, Eline K. R. de Meyer. ✉e-mail: s.slingerland@umcg.nl

pronounced reductions to similar or even paradoxically increased dopaminergic signal[17]. There is a lack of data based on simultaneously assessed cholinergic and dopaminergic changes in GBA-PD and their association with clinical phenotypes[17]. This study used 3,4-dihydroxy-6-18F-fluoro-I-phenylalanine (^{18}F-FDOPA) PET to quantify dopaminergic striatal presynaptic integrity in vivo[18].

In the present study, we examined the effect of *GBA1* carrier status on the progression of clinical features, related to cholinergic as well as dopaminergic innervation changes in PD. We hypothesized that the GBA-PD phenotype is primarily driven by cholinergic more than dopaminergic decline.

Results

Demographic and clinical characteristics

In total, 170 PD patients (of which 118 de novo; 124 male), with a mean age of 65.2 ± 8.7 years were included in the ^{18}F-FEOBV analysis. See Supplementary Table 1 for an overview of all included patients. Demographic and clinical data of GBA-PD (n = 44) and non-GBA-PD (n = 126) subjects are presented in Table 1 and Fig. 1. See Supplementary Table 2 for the corresponding fixed effects from the linear mixed-model. The GBA-PD group had a significantly longer time since diagnosis than the non-GBA-PD group (4.5 ± 1.7 *vs.* 3.2 ± 1.9 years). GBA-PD patients performed significantly worse on the cognitive domain 'executive function' compared to non-GBA-PD. Over time, significant increases were found for the MDS-UPDRS III total score, NMS-Quest total score (which means more non-motor symptoms over time) and T-scores of the memory domain, irrespective of *GBA1* carriers status. Lastly, there was a significant interaction between *GBA1* status and time, where GBA-PD had a faster progression of Hoehn and Yahr scores compared to non-GBA-PD over time.

In total, 135 PD patients (of which 120 de novo PD; 100 male) were included in the ^{18}F-FDOPA analysis, with a mean age of 64.9 ± 9.1 years. Only the non-GBA-PD patients belonging to the DUPARC cohort had ^{18}F-FDOPA imaging at BL and follow-up. The GBA-PD group (n = 26) had a significantly longer time since diagnosis than non-GBA-PD (n = 109). Over time, a significant increase in MDS-UPDRS III total score, increase in NMS-Quest total score, and HADS depression score and RBD-Q total score was found, irrespective of *GBA1* status. A significant interaction between *GBA1* status and time was found for the MDS-UPDRS III, in which GBA-PD had a faster increase in motor symptoms compared to non-GBA-PD. See Table 2, Supplementary Fig. 1 and Supplementary Table 3. See Supplementary Table 4 for the corresponding fixed effects from the linear mixed-model for the clinical data of patients included in the ^{18}F-FDOPA analysis.

Cholinergic innervation changes over time

The ^{18}F-FEOBV imaging showed a significant main effect in a cluster at the right precentral and middle frontal gyrus, with lower binding in patients with *GBA1* relative to non-GBA (3640 µL), (see Fig. 2A). In a post-hoc

Table 1 | Demographic and clinical characteristics of study participants included in ^{18}F-FEOBV analysis

	GBA-PD, (n = 44)	non-GBA-PD, (n = 126)	P-value Group	P-value Time	P-value Group x Time
Demographics					
Age, years (mean (SD))	68.27 (8.1)	66.61 (9.0)	0.260		
Age at disease onset, *y*	63.75 (8.3)	63.59 (9.3)	0.912		
Gender, male *n* (%male)	27 (61.4%)	96 (77.0%)	0.065		
Educational level [median, Q1–Q3]	5.00 [4.25-6.00]	5.00 [4.00-6.00]	0.574		
Anticholinergic drug use, *n* (%)	5 (11.4%)	3 (2.4%)	0.080		
Time since diagnosis, *y*	4.47 (1.7)	3.18 (1.9)	**<0.001**		
Clinical characteristics					
Motor symptoms					
MDS-UPDRS-III	30.84 (12.7)	30.07 (10.6)[a]	0.671	**0.001**	0.061
Hoehn and Yahr stage	2.00 [2.00–2.00]	2.00 [2.00–2.00]	0.445	0.528	**0.044**
Non-motor symptoms					
MoCA, total score	26.00 [23.00–27.00]	26.00 [24.00–27.75]	0.472	0.366	0.770
NMS-Quest, total score	8.00 [5.00–12.00][b]	5.00 [3.00–9.00][c]	0.915	**0.007**	0.295
HADS anxiety, total score	4.00 [2.00–7.00][d]	4.00 [2.00–6.00][e]	0.473	0.059	0.066
HADS depression, total score	4.00 [2.00–6.00][d]	3.00 [1.00–6.00][e]	0.707	0.206	0.363
RBD Quest, total score	6.00 [2.50–8.50][a]	3.00 [2.00–6.00][f]	0.449	**0.017**	0.572
Cognitive performance					
T-score memory	45.81 (7.9)	47.12 (7.0)	0.806	**0.006**	0.187
T-score attention	39.46 (9.4)	43.03 (7.5)[a]	0.521	0.413	0.113
T-score executive function	42.42 (9.8)	46.69 (8.2)	**0.041**	0.646	0.746
T-score language	46.17 (10.1)[a]	50.22 (8.9)[d]	0.177	0.921	0.967
T-score visuospatial function	43.68 (13.2)	45.81 (11.7)[e]	0.923	0.802	0.549

For participants with data at two time points, baseline assessments were used to present the clinical data of GBA-PD and non-GBA-PD.
Educational level according to the Dutch Verhage scale, *HADS* Anxiety and Depression Scale, *MDS-UPDRS III* Movement Disorders Society Unified Parkinson's Disease Rating Scale part III, *MoCA* Montreal Cognitive Assessment, *NMS-Quest* Non-Motor Symptoms Questionnaire, *RBD Quest* NMS-REM Sleep Behavior Disorder Screening Questionnaire.
[a]Missing = 1.
[b]Missing n = 3.
[c]Missing n = 25.
[d]Missing n = 5.
[e]Missing n = 4.
[f]Missing n = 2.

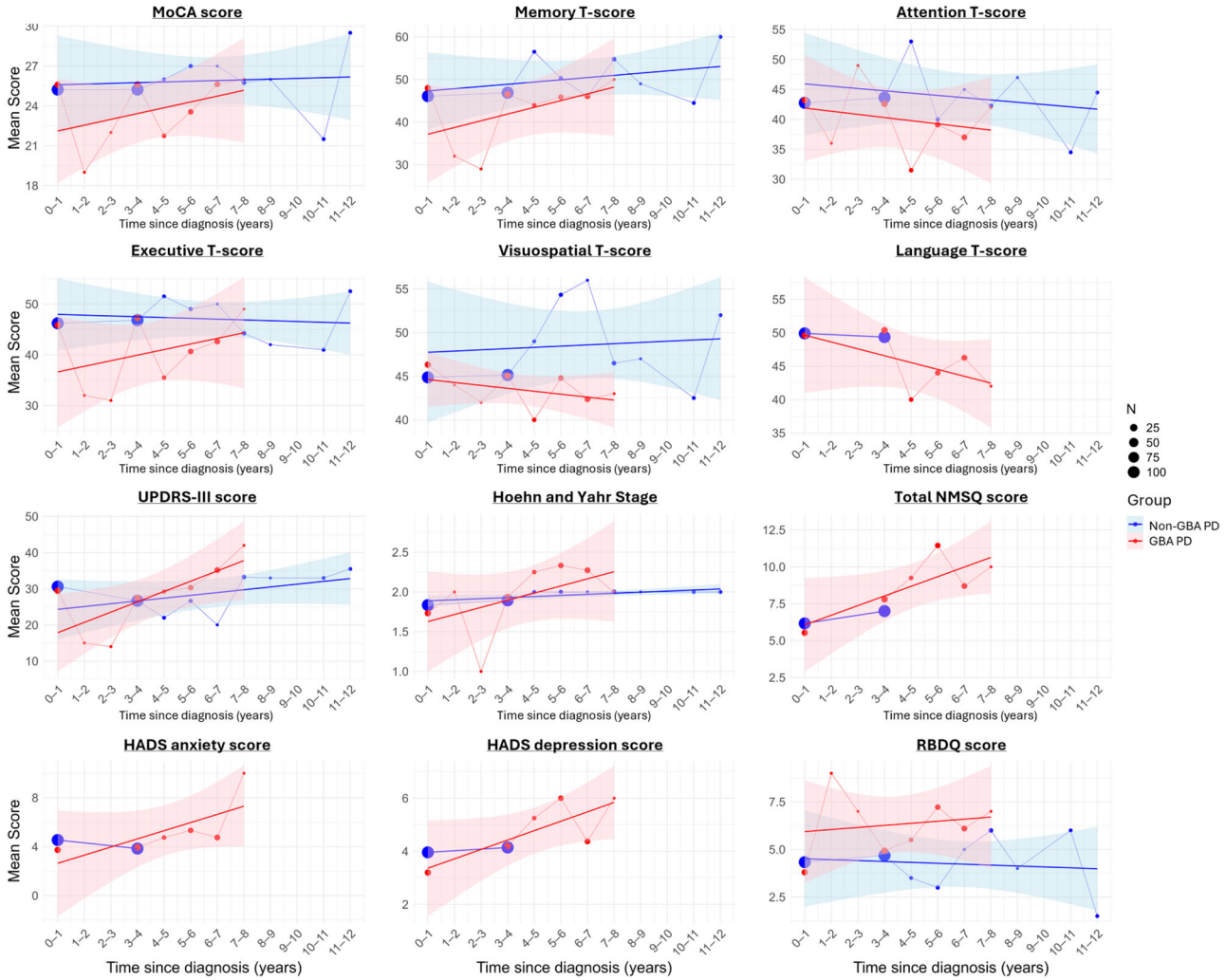

Fig. 1 | Trajectories of clinical data over time of Parkinson's disease participants with a *GBA1* variant (GBA-PD, $n = 44$) and Parkinson's disease participants without a *GBA1* variant (non-GBA-PD, $n = 126$) including in ^{18}F-FEOBV analysis. For each variable, the figure shows mean scores over time since diagnosis (years) for the two groups (red = GBA-PD, blue = non-GBA-PD). Thin lines connect the mean points, and shaded areas show 95% confidence intervals from linear regression models fitted to the raw data.

Table 2 | Demographic and clinical characteristics of study participants included in ^{18}F-FDOPA analysis

	GBA-PD, ($n = 26$)	Non-GBA-PD, ($n = 109$)	*P* value Group
Demographics			
Age, years (mean(SD))	66.42 (9.8)	64.57 (8.9)	0.385
Age at disease onset, years	64.20 (9.5)	64.57 (8.9)	0.859
Gender, male n (%male)	18 (69.2%)	82 (75.2%)	0.557
Educational level [median, Q1-Q3]	5.00 [4.00-6.00]	5.00 [4.00-6.00]	0.793
Anticholinergic drug use, n (%)	3 (11.5%)	0 (0.0%)	0.083
Time since diagnosis, years	2.22 (2.73)	0.11 (0.057)	**<0.001**

For participants with data at two time points, baseline assessments were used to present the demographic data of GBA-PD and non-GBA-PD.

analysis, we fitted a linear mixed-effects model with mean ^{18}F-FEOBV uptake in this cluster as the dependent variable and time since diagnosis, age, sex, and a random intercept for subject as predictor, thus excluding the group effect from the analysis. This resulted in a lower mean and reduced variance for GBA-PD compared to non-GBA-PD. These findings confirm that this cluster shows an effect of GBA status on ^{18}F-FEOBV uptake, which cannot be explained by time since diagnosis, age or gender. (see Fig. 2B). Exploratory analyses examining the relationship between mean ^{18}F-FEOBV DVR value in this cluster and cognitive performance are reported in Supplementary Fig. 2, showing a significant positive relationships with the T-scores of all cognitive domains, corrected for age and gender.

A cluster of widespread cholinergic denervation (lower binding over time) of cortical, subcortical, and limbic regions was observed for the main effect of time since diagnosis (1,099,440 µL). The largest F values were found in posterior regions, including the bilateral (pre)cuneus, insula, posterior cingulate, transverse temporal gyrus, superior temporal gyrus, pre- and postcentral gyrus, and the lateral posterior nucleus of the thalamus (see Fig. 3A). No clusters were identified for the Group x Time interaction. This indicates that across all timepoints, GBA-PD had consistently lower ^{18}F-FEOBV binding in areas of the frontal cortex, but not a faster rate of decline. A plot visualized the progression of ^{18}F-FEOBV binding in the significant cluster between baseline and follow-up in our de novo cohort (Fig. 3B).

A significant widespread cluster of cholinergic cortical and subcortical denervation was associated with the effect of age (1,273,448 µL). In contrast to the effect of time, the most robust F-values for age were observed in anterior regions, including the anterior cingulate, insula, and precentral gyrus, parahippocampal gyrus, pons, caudate and medial dorsal thalamus (Fig. 4A). Higher mean ^{18}F-FEOBV uptake found within the *age* cluster was

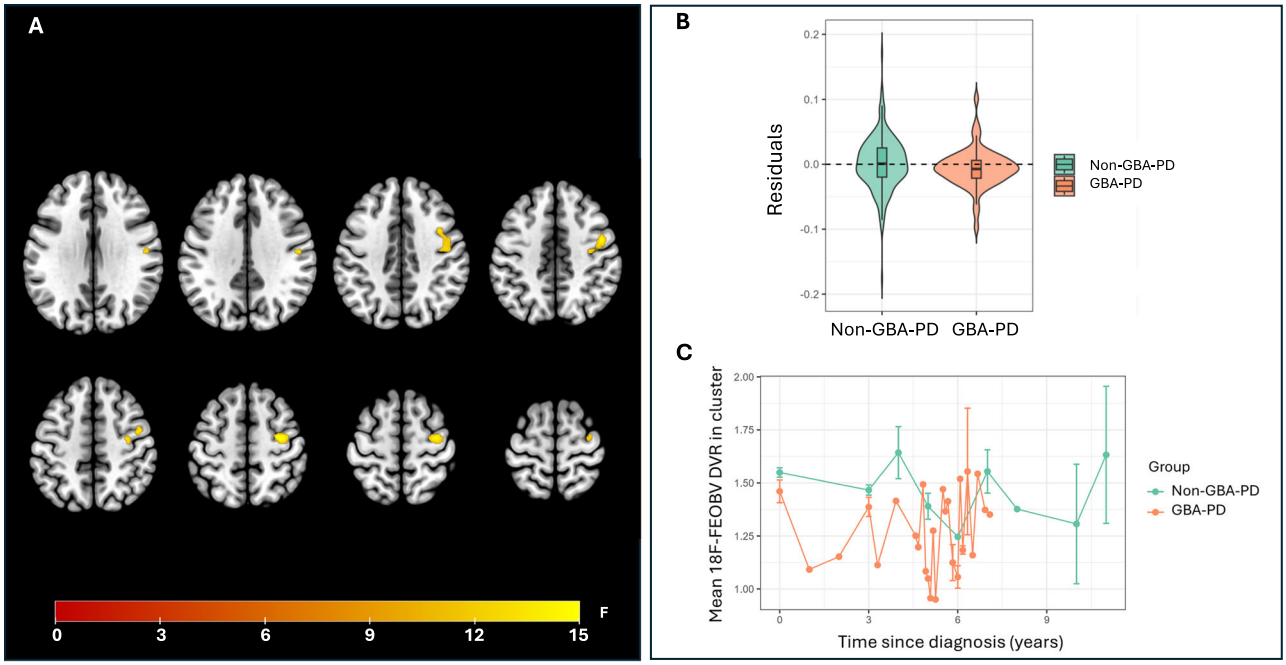

Fig. 2 | Results from the linear mixed model comparing Parkinson's disease with a GBA1 variant (GBA-PD) to Parkinson's disease without a *GBA1* variant (non-GBA-PD. Left (**A**): Voxel-wise results from the linear mixed model comparing Parkinson's disease with a *GBA1* variant (GBA-PD) to Parkinson's disease without a *GBA1* variant (non-GBA-PD). A significant main group effect was observed, showing a cluster of reduced ^{18}F-FEOBV binding in the right precentral and middle frontal gyri in the GBA-PD group. Right (**B**): Boxplot of the residuals from a linear mixed-effects model for mean ^{18}F-FEOBV uptake in this cluster with time since diagnosis, age, sex, and a random intercept for subject-level as a predictor. **C** Group-level trajectories of mean ^{18}F-FEOBV uptake in this cluster across time. The line plot shows mean values (± standard error) for each group at different time points.

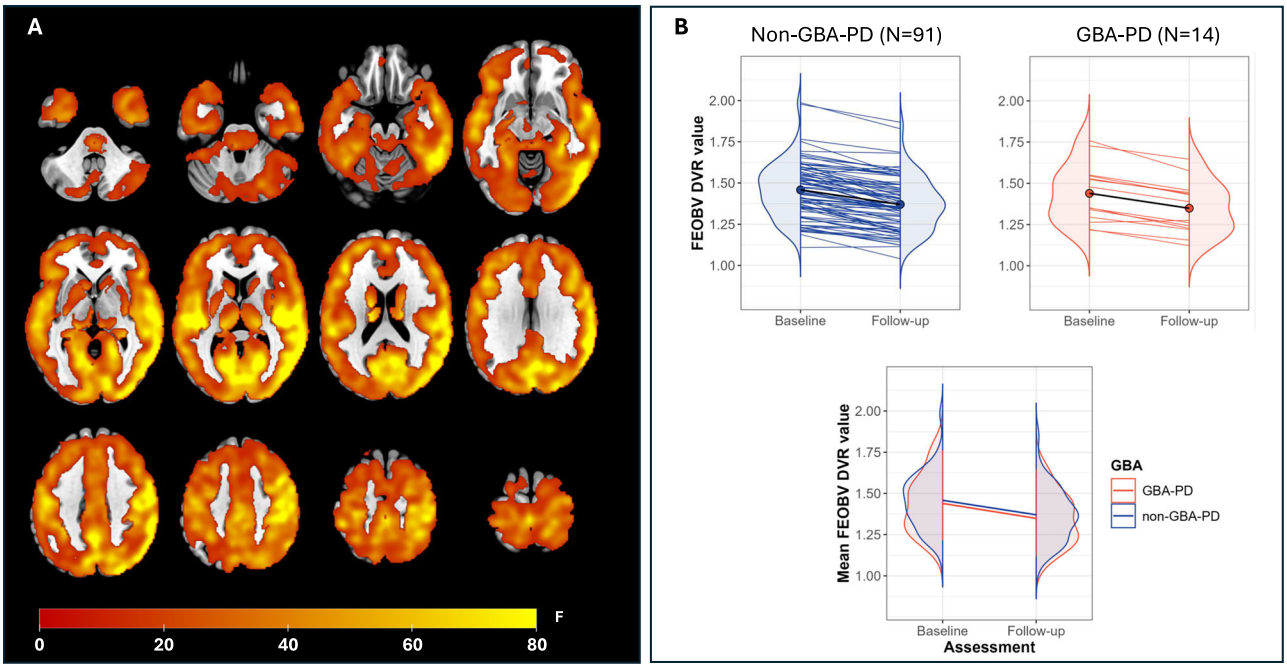

Fig. 3 | ^{18}F-FEOBV results from the linear mixed model for the effect of Time. Left (**A**): Voxel-wise results from the linear mixed model showing a widespread significant cluster of decreased ^{18}F-FEOBV binding over time. Right (**B**): Mean ^{18}F-FEOBV Distribution Volume Ratio (DVR) within this time-sensitive cluster at baseline and follow-up in participants who were de novo at baseline and had both an assessment at baseline and after three years, illustrating longitudinal decline in cholinergic binding.

associated with younger age (see Supplementary Fig. 3). A significant main effect of sex was found. In this cluster (850,280 µL), males showed diffusely lower cholinergic binding compared to females. The largest sex-related F-values were observed in subcortical regions, including the bilateral lentiform nucleus, caudate, parahippocampal gyrus, and insula (see Fig. 4B).

Dopaminergic innervation changes over time

There was a significant main effect of time (decrease) within a cluster in the bilateral striatum (32,216 µL) (see Figs. 5A and 6). Conversely, a cluster with significant increase in ^{18}F-FDOPA uptake was found in the cerebellum (11,672 µL) (see Fig. 5A and Supplementary Fig. 4).

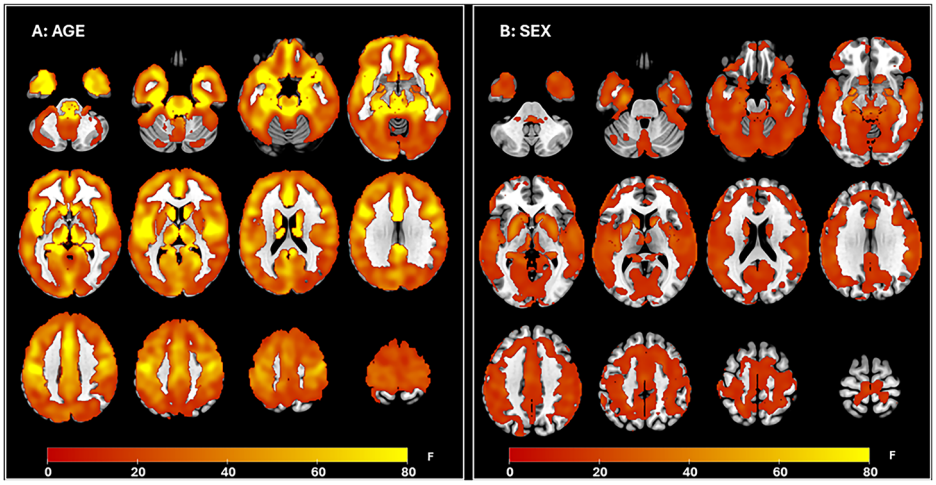

Fig. 4 | ^{18}F-FEOBV voxel-wise results from the linear mixed model for the effect of Age and Sex. Voxel-wise results from the linear mixed model showing a significant cluster of ^{18}F-FEOBV binding associated with the effect of age (**A**) and a separate significant cluster associated with the effect of sex (**B**). **A** Within the age-related cluster, lower mean ^{18}F-FEOBV uptake was associated with older age. **B** Within the sex-related cluster, males exhibited diffusely lower cholinergic binding compared to females.

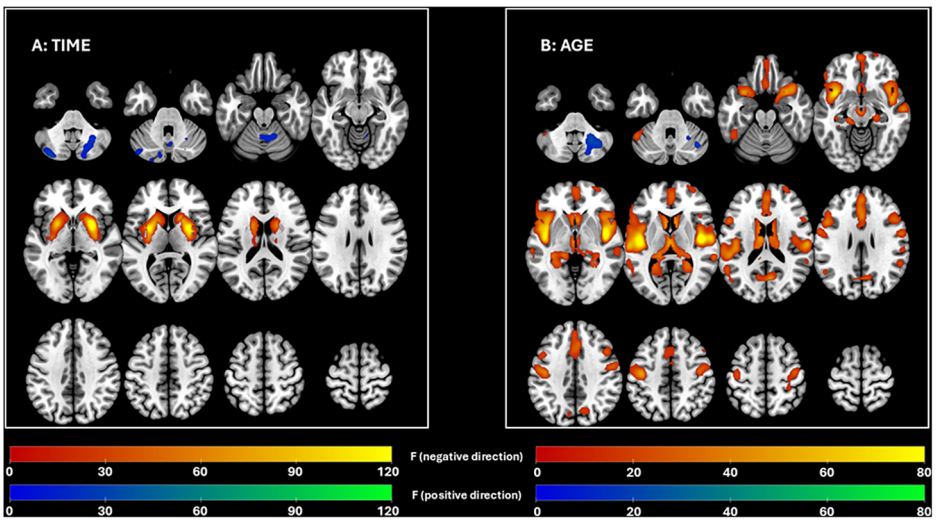

Fig. 5 | ^{18}F-FDOPA voxel-wise results from the linear mixed model for the effect of Time and Age. Voxel-wise results from the linear mixed model showing significant clusters of ^{18}F-FDOPA binding associated with the effect of time (**A**), and separate significant clusters associated with the effect of age (**B**). Red–yellow colors represent F-values corresponding to decreases in ^{18}F-FDOPA uptake (negative direction), while blue–green colors represent F-values corresponding to increases in uptake (positive direction).

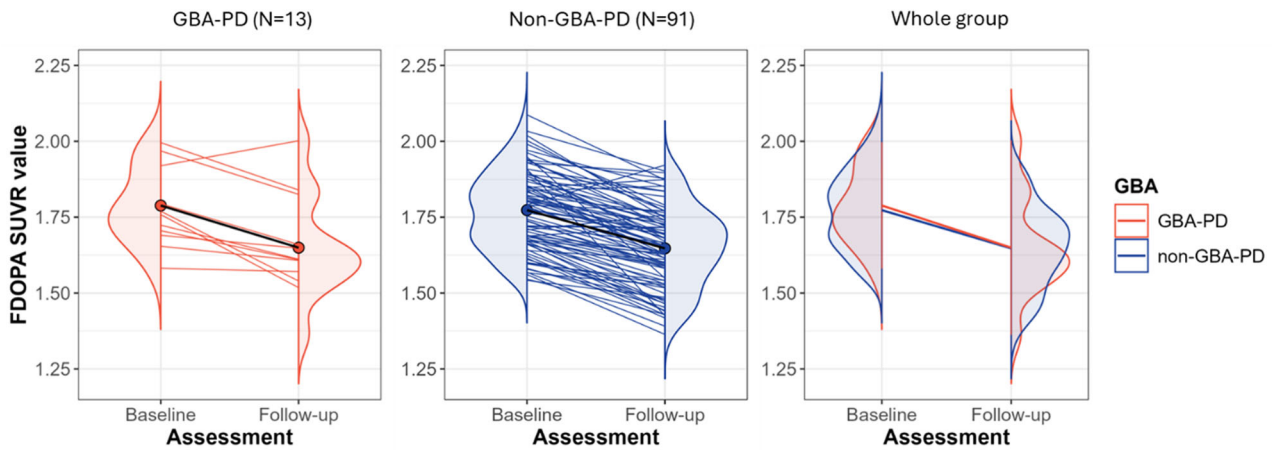

Fig. 6 | Mean ^{18}F-FDOPA Standard Uptake Values (SUVR) in the striatum at Baseline and Follow-up. Mean ^{18}F-FDOPA Standard Uptake Values (SUVR) in the striatum at Baseline and Follow-up in participants who were de novo at baseline and had both an assessment at baseline and after 3 years.

No significant differences in ^{18}F-FDOPA uptake distribution were observed between GBA-PD or non-GBA-PD. In addition, there were no significant clusters identified for the Group x Time interaction.

Ten clusters were found where age had a significant effect on ^{18}F-FDOPA signal. Older age was significantly associated with reduced ^{18}F-FDOPA uptake across various cerebral regions (with a total cluster volume of 180,064 µL) (see Fig. 5B). The most robust age-related declines were observed in the bilateral insula/operculum. Substantial reductions were also evident in subcortical structures, including the bilateral caudate and thalamus. Cortical areas, predominantly within the prefrontal cortex and

cingulate cortex, also demonstrated this negative association. Additionally, smaller clusters in lateral frontal, parietal and temporal regions exhibited similar age-related decreases in ^{18}F-FDOPA uptake. In contrast, older age was also associated with increased ^{18}F-FDOPA uptake in a cluster in the cerebellum (6576 μL). A more detailed overview of the significant clusters, and their relationship to age, can be found in the Supplementary Materials see Supplementary Fig. 5, Supplementary Table 5 and Supplementary Fig. 6.

There was no significant effect of sex on ^{18}F-FDOPA brain distribution.

Sensitivity analyses

The 104 de novo PD patients with a follow-up assessment (79 male) had a mean age of 64.5 ± 9.5 years at baseline. Demographic and clinical data of GBA-PD (n = 14), non-GBA-PD (n = 90) of subjects included in ^{18}F-FEOBV analysis are presented in Supplementary Table 6. We did not find any differences in demographic -, motor -, non-motor - and cognitive characteristics at both baseline and FU3 between GBA-PD and non-GBA-PD. In addition, no significant difference in ΔT-scores of the cognitive domains were found between GBA-PD and non-GBA-PD. At baseline four patients (28.6%) and at FU3 five patients (35.7%) were characterized as MCI in the GBA-PD group (p = 0.164), compared to, respectively, 40 (44.4%) and 41 (45.6%) in the non-GBA-PD group (p = 0.516). Within group comparisons revealed no statistically significant difference in T-scores between baseline and FU3 in both GBA-PD and non-GBA-PD. In this subsample, the voxel-wise analyses revealed no significant clusters for the effect of Group in either the ^{18}F-FEOBV or ^{18}F-FDOPA models. Consistent with the main analysis including all cohorts, no significant clusters were observed for the Group × Time interaction. The effect of Time was similar to that observed in the full sample. Results of the sensitivity analyses of the voxel-wise linear mixed model for ^{18}F-FEOBV PET and ^{18}F-FDOPA PET are shown in Supplementary Fig. 7.

Discussion

We studied the progression of clinical features, as well as the cholinergic and dopaminergic changes in GBA-PD compared to non-GBA-PD. To the best of our knowledge, this is the first longitudinal dual neurotransmitter change description in GBA-PD patients.

GBA-PD exhibited poorer executive functioning compared to non-GBA-PD. However, no differences in cognitive deterioration were observed between GBA-PD and non-GBA-PD in our cohort with PD patients. This finding aligns with previous studies that assessed cognitive changes over a longer time period, showing that the rate of decline of GBA-PD compared to non-GBA PD started to differ approximately 3 years post- diagnosis[3,6,19].

The voxel-wise linear mixed model with ^{18}F-FEOBV uptake revealed a modest significant lower cholinergic innervation in GBA-PD at the right precentral gyrus and in the middle frontal gyrus. Previous studies have linked cortical cholinergic denervation to cognitive impairment in PD[20–22]. In addition, another study demonstrated that early frontal cholinergic denervation is associated with cognitive decline in PD[7]. This corresponds to our finding that GBA-PD performed worse on executive functioning compared to non-GBA-PD.

We did not find significant differences in cognitive characteristics between GBA-PD and non-GBA-PD patients of patients included in the ^{18}F-FDOPA analyses. In addition, ^{18}F-FDOPA PET evaluation demonstrated no significant regions with higher or lower striatal dopaminergic binding, comparing GBA-PD to non-GBA-PD, which is consistent with other studies[18,23,24]. Early executive dysfunction is also related to dopaminergic modulation of the frontal-striatal system, whereas reduced ^{18}F-FDOPA uptake in the caudate nucleus and frontal cortex is associated with impairment in working memory and attentional functioning[25]. We did not observe such associations in our cohort. In contrast, a previous study also using ^{18}F-FDOPA PET reported more pronounced dopaminergic deficits in GBA-PD at the bilateral caudate nuclei, the ipsilateral antero-medial putamen, and nucleus accumbens, contralateral to the more affected body side. Notably, the GBA-PD group in that study also showed worse global cognitive performances compared to non-GBA-PD, which may explain the discrepancy[26]. Another study examined the progression of dopamine transporter (DAT) levels in early GBA-PD patients and found lower DAT levels in the ventral striatum along with more severe cognitive symptoms. Interestingly, after two years, DAT binding became comparable to early-onset non-GBA-PD patients[27]. While ^{18}F-FDOPA PET is converted by aromatic L-amino acid decarboxylase (AADC) to dopamine in dopaminergic neurons and thus reflects dopamine synthesis and storage capacity[28]. In contrast, DAT imaging measures the availability of dopamine transporters, which are involved in dopamine reuptake[29]. In early disease stages, dopamine transporters are thought to be downregulated, while AADC is thought to be upregulated[30]. Discrepancies between DAT and ^{18}F-FDOPA imaging findings could partially be attributed to differences in the biological substrates (binding sites) targeted by the respective radiotracers.

Although our results revealed an overall reduced cholinergic innervation in frontal regions in GBA-PD compared to non-GBA-PD, we did not observe an interaction effect of *GBA1* status and time. This may indicate an earlier onset of cholinergic degeneration in GBA-PD, rather than a similar progression rate between groups. This aligns with our clinical findings, not showing any difference in cognitive deterioration between GBA- and non-GBA PD over time. Similarly, the voxel-wise linear mixed-model of ^{18}F-FDOPA revealed no interaction effect of *GBA1* variants and time, indicating a comparable progression of dopaminergic degeneration in GBA-PD and non-GBA-PD within our relatively short follow-up of 3 years. Therefore, we suggest that the decline in cholinergic and dopaminergic innervation might become different between GBA-PD and non-GBA-PD in the later stages of the disease, corresponding with the more pronounced clinical symptoms observed in GBA-PD after longer observation periods, being part of its distinct phenotype[3–6]. For an overview of the hypothesized sequence of neurodegenerative changes in *GBA1*-related PD based on our data, see Supplementary Fig. 8.

Cholinergic denervation was most strongly related to time in the posterior regions, involving the bilateral (pre)cuneus, insula, posterior cingulate, transverse temporal gyrus, superior temporal gyrus, pre- and postcentral gyrus. This is in line with previous studies reporting the cholinergic denervation pattern in sporadic PD[7,31–34]. Posterior cholinergic denervation is also present in non-demented PD[22] and might even be present before PD diagnosis[35]. Other studies showed that posterior cholinergic loss did not correlate significantly with cognitive outcomes[36,37]. Clinical impairment seemed to be more related to limbic and more anterior located regions. Previous cross-sectional imaging results suggested a posterior-to-anterior gradient of cortical cholinergic denervation, when PD progressed to PDD[9,34]. Our previous study on de novo PD also demonstrated more extensive posterior cholinergic denervation in GBA-PD, compared to age- and sex-matched non-GBA-PD, when compared to controls[16]. In this current study, GBA-PD showed more prominent involvement of frontal regions compared to non-GBA-PD, independent of time since diagnosis, age or gender. These results suggest that GBA-PD might be further along this denervation process than non-GBA-PD, which may contribute to the *GBA1*-linked phenotype, contributing to greater cognitive vulnerability.

Advancing age was associated with differences in cholinergic denervation, with the strongest effects observed in anterior brain regions. A prior PET study assessing longitudinal changes in cortical cholinergic activity in PD found the most severe denervation in posterior regions at baseline, followed by progressive involvement of anterior regions over time—suggesting an anterior-to-posterior degeneration pattern[34]. Advancing age may reflect individuals further along this degenerative trajectory. Our finding that older age is most strongly linked to anterior cholinergic denervation—regions critical for cognitive function[7] —may therefore reflect a later stage in the global cholinergic degeneration process. In this context, posterior regions may have already undergone near-complete denervation in older individuals, resulting in a floor effect that limits the detectable variance in these areas, thereby enhancing the apparent association with anterior regions. This may help explain why advancing age is a known predictor of cognitive impairment and increased risk of PDD[38–40].

The relationship between age and ^{18}F-FDOPA imaging is not fully understood. While some studies[41] have reported age-related decreases in

striatal ^{18}F-FDOPA uptake, others did not observe this effect[42]. In our study, we identified a significant age-related reduction in ^{18}F-FDOPA uptake, not only in the caudate, but also in extra-striatal regions, including midbrain, prefrontal cortex, and cingulate cortex, as well as regions like the insula and cortical areas in the temporal and parietal lobe. Interestingly, advancing age was associated with higher ^{18}F-FDOPA signal in the cerebellum, a region often used as a reference region in presynaptic dopaminergic imaging due to its minimal dopaminergic activity. ^{18}F-FDOPA does not solely reflect dopaminergic brain innervation but is also taken up in non-dopaminergic neurons where it is decarboxylated in serotonin and noradrenaline[43]. This widespread pattern suggests that aging impacts both dopaminergic and broader monoaminergic neurotransmission across diverse brain networks. Our findings are similar to another study, which investigated the relationship between age and ^{18}F-FDOPA uptake index in healthy volunteers[44]. These findings could also be partially influenced by normal age-related brain atrophy, independent of PD[44].

Lastly, male sex has often been reported as risk factor in developing MCI in PD, suggesting a faster trajectory of cognitive decline[45]. Accordingly, a different cholinergic topography may be expected. Indeed, a previous study demonstrated greater cortical cholinergic denervation in male PD patients[46] In addition, while other studies showed that females have higher dopaminergic innervation, especially in the caudate and prefrontal cortex[46,47], sex did not contribute significantly to ^{18}F-FDOPA brain uptake in our linear mixed model analysis. Both biological and methodological differences could be responsible for the discrepancy between the ^{18}F-FEOBV and ^{18}F-FDOPA results. ^{18}F-FEOBV binds to the vesicular acetylcholine transporter and provides a direct measure of cholinergic integrity with a high signal-to-noise ratio in cortical regions[15]. Contrastingly, ^{18}F-FDOPA serves as an indirect measure for dopaminergic integrity by reflecting dopamine synthesis capacity through L-amino acid decarboxylase activity. This system can be influenced by compensatory mechanisms and small differences in dopaminergic denervation could be masked[48]. Furthermore, the sensitivity of ^{18}F-FDOPA PET to detect variations in monoaminergic innervation outside of the striatum is limited by its low signal-to-noise ratio in extrastriatal areas[49].

This study presents detailed subject assessments, including extensive neuropsychological test battery, motor and nonmotor assessments, and dual-tracer PET imaging with ^{18}F-FDOPA PET and ^{18}F-FEOBV PET. As far as we know, 3dLME is the only voxel-wise analysis software that supports specifying multiple types of variance-covariance structures. A final strength is the use of full-gene *GBA*1 sequencing. A limitation of this study is the relatively small sample size of the GBA-PD group. To compensate this, data from an additional cross-sectional cohort was included, which provided a larger number of GBA-PD participants and thereby increase statistical power. However, despite these efforts there is still a significant imbalance between the number of participants with GBA-PD and non-GBA-PD, which still may affect the reliability of the model and future studies should ideally include larger, prospectively followed and more balanced *GBA1*-genotyped cohorts to validate and refine these findings. In addition, a comprehensive assessment of motor progression was limited, because the motor scores were assessed in the dopaminergic "on" state following treatment initiation. Nevertheless, our results align with previous research that reported an increased rate of motor progression in GBA-PD[3–5,50]. The discrepancy between on/off state may, however, have also influenced performance on the cognitive tests. Finally, a potential limitation of this study could be that the effect of age at disease onset was not examined separately, as this may interact with disease progression. However, the use of type III sums of squares means that both age and time since diagnosis were included in the model, indirectly accounting for this factor. Moreover, there was no significant difference in age-at-onset between GBA-PD and non-GBA-PD participants.

This study investigated the clinical phenotype together with both dopaminergic and cholinergic denervation changes over time in PD patients, with and without *GBA1* mutations. The results revealed reduced cholinergic innervation in the right precentral gyrus and middle frontal gyrus in individuals with *GBA1* variants, compared to those with non-GBA-PD, although the rate of progression of cholinergic degeneration did not differ between both groups. Additionally, no differences were found in striatal dopaminergic denervation between GBA-PD and non-GBA-PD subjects. Studies with larger sample sizes and extended follow-up duration are needed to determine whether ^{18}F-FEOBV PET, besides ^{18}F-FDOPA PET, can serve as a biomarker to measure disease progression in GBA-PD.

Methods

Setting and participants

We collected data of 171 PD patients (44 GBA-PD and 128 non-GBA-PD). For an overview of included patients, see supplementary material Supplementary Table 1. The majority of the patients (a total of 127 participants of whom 15 were *GBA1* carriers) were enrolled via the Dutch Parkinson Cohort (DUPARC) study[51]. This study included de novo treatment-naïve PD patients with a follow-up evaluation three years post diagnosis (FU3), conducted within a time frame of 35 to 39 months after baseline assessments. At FU3, 113 patients (14 GBA-PD and 98 non-GBA-PD) underwent ^{18}F-FEOBV PET and, 109 participants (13 GBA-PD and 96 non-GBA-PD) underwent ^{18}F-FDOPA PET scan.

Because of the large imbalance between the number of GBA-PD and non-GBA-PD participants within the DUPARC cohort, with only 15 GBA-PD patients, additional participants were recruited via two other ongoing studies within our research group, adhering to the same clinical and imaging protocols (n = 44, 29 GBA-PD and 15 non-GBA-PD)[52,53]. These PD patients had a varying duration of disease (mean duration of 3.7 ± 1.9 years with a maximum duration of 11 years) and had clinical and imaging assessments once. In total, 170 subjects underwent ^{18}F-FEOBV PET, and 136 subjects with a ^{18}F-FDOPA PET scan.

All patients met the criteria for PD diagnosis according to the Movement Disorder Society (MDS) Clinical Diagnostic Criteria for PD[54]. Patients underwent a standardized clinical and neuropsychological examination, a T1-weighted MRI scan, ^{18}F-FEOBV PET and/or ^{18}F-FDOPA PET. Exclusion criteria included inability to provide written informed consent, estimated low premorbid intelligence level (estimated IQ < 70 on the Dutch Adult Reading test)[55] and MRI contra-indications (e.g. ferrous objects in the body or claustrophobia). All subjects provided written informed consent in accordance with the Declaration of Helsinki and the study was conducted according to the Good Clinical Practice guidelines. The study was approved by the ethical board of the University Medical Center Groningen.

Genotyping

We collected saliva samples from PD subjects using Oragene DNA OG-500 tubes (DNA Genotek). DNA extraction, whole *GBA1*-gene sequencing and data analysis were carried out by GenomeScan B.V. in Leiden, the Netherlands. To ensure specific sequencing of the functional *GBA1*-gene rather than its pseudogene, long-range PCR was employed to select primers. Subsequently, DNA fragments were amplified using PCR and sequencing was performed using Illumina cBot and HiSeq 400, as described previously[56]. The allelic nomenclature of the *GBA1* variants is given in Supplementary Table 7.

Clinical assessment

All PD participants had a neuropsychological test battery (see Supplementary Table 8 for details) covering the 5 main cognitive domains; memory, attention, executive functions, language, visuospatial function. All (sub)test scores were transformed into standardized T-scores based on established test-specific normative data. T-scores within a cognitive domain were averaged to define a domain-specific T-score for each domain. Test scores for the Boston naming test and the Location Learning test were transformed into standardized T-scores based on a sample of 108 controls (58 males, aging ranges between 41 and 84 years; mean age = 64.49 years, SD = 8.08 years) collected as part of the DUPARC study. All T-scores within one cognitive domain were averaged to define a domain-specific T-score for each of the 5 domains. A selection of outcome measures of tests and subtests of the cognitive test battery was made a priori, allowing implementation of level II criteria for Parkinson's disease with mild cognitive impairment

(PD-MCI, see Supplementary Table 8). Below-threshold performance on at least two neuropsychological tests was required for PD-MCI classification. Scores >1.5 SD below normative values were considered abnormal[57,58]. To define Parkinson's disease dementia (PDD) we used the MDS Clinical Diagnostic Criteria[59]. Below-threshold performance on test or subtests in more than one cognitive domains was required. A selection of outcome measures of test and subtests of the cognitive test battery was made a prior, see S3. Scores >1.5 SD below normative values were considered abnormal. If one of the tests per domain was below the threshold, the domain was scored as abnormal. In addition, one of the behavioural features (1) apathy, 2) changes in personality and mood including depressive features and anxiety 3) hallucinations, 4) delusions and 5) excessive daytime sleepiness is present assessed by the NMS-Q at follow-up. Since one of the core features is that there is a representing decline from premorbid level we applied this criteria to the patients that underwent two assessments to observe the difference between baseline and follow-up.

For each cognitive domain, the difference in performance over the 3-year interval was obtained for the participants that underwent both baseline and FU3 measurements as follows:

$$\Delta\text{TCognitive domain} = (\text{T} - \text{score follow} - \text{up}) - (\text{T} - \text{score baseline})$$

The ΔTCognitive domain scores represents cognitive changes over time, with positive scores representing an improvement and negative scores a decline.

Clinical motor performance was examined using the MDS-revised Unified Parkinson's Disease Rating Scale part III (MDS-UPDRS-III). De novo patients at baseline were treatment-naïve and therefore scored in "off" state. After treatment initiation (i.e., in non-de novo subjects), all clinical assessments were performed in the dopaminergic "on" state and the Levodopa Equivalent Daily Dose (LEDD) was calculated[60].

Presence of non-motor symptoms was assessed using the Hospital Anxiety and Depression Scale, Non-Motor Symptoms Questionnaire (NMS-Q) and REM Sleep Behavior Disorder Screening Questionnaire (RBD-Q)[51].

Acquisition procedures of ^{18}F-FEOBV and ^{18}F-FDOPA

Participants underwent brain magnetic resonance imaging (MRI), ^{18}F-FDOPA imaging and/or ^{18}F-FEOBV. All subjects underwent brain MRI, ^{18}F-FDOPA PET and ^{18}F-FEOBV PET. MRI imaging of Parkinson's disease subjects was acquired using Siemens Magnetom Prisma 3-Tesla magnetic resonance imaging scanners (Best, Netherlands), equipped with SENSE-8 channel head coil. For each subject, anatomical T1-weighted images were obtained using a sagittal 3-dimensional gradient-echo T1 weighted sequence with 0.9 × 0.9 × 0.9 mm acquisition. [^{18}F]FEOBV imaging was performed on the same day as MR imaging. For PET imaging, participants first underwent lose-dose computed tomography (CT) for attenuation and scatter correction using either a Biograph 40-mCT or 64-mCT (Siemens Healthcare, USA). Both scanners were EARL certified, had the same software version, and used identical acquisition and reconstruction protocols and PET detectors. Thirty minute scans (in six 5-minute frames) were acquired at 210 min post-bolus injection of ^{18}F-FEOBV. ^{18}F-FDOPA PET was performed after at least six hours of fasting (four hours for diabetic patients). Participants were premedicated with carbidopa 60 min before receiving 200MBq of the FDOPA tracer, 90 min after which the PET-scan was performed with a static acquisition lasting 6 min.

Pre-processing of ^{18}F-FEOBV and ^{18}F-FDOPA imaging

The six five-minute ^{18}F-FEOBV PET image frames were realigned within subjects to reduce the effect of subject motion during imaging session using Statistical Parametric Mapping (SPM12; Wellcome Trust Centre for Neuroimaging, London, UK). PET-MRI registration was performed using T1-weighted MRI volumetric scans with SPM for ^{18}F-FEOBV and PMOD version 3.8 (Bruker Preclinical Imaging, Switzerland), for ^{18}F-FDOPA. Parametric ^{18}F-FEOBV brain images reflecting Distribution Volume Ratios (DVR) were constructed, using the supratentorial white matter above the ventricles as a reference region. This region was delineated based on segmentation of the T1-weighted MRI with Freesurfer software (Laboratory for Computational Neuroimaging, Athinoula A. Martinos Center for Biomedical Imaging, Boston, MA), using the recon-all function, as previous described[61] and was morphologically eroded. Raw ^{18}F-FEOBV PET values of this reference region were extracted for each participant. DVR maps were computed using SPM's ImCalc function, dividing voxel-wise PET signal by the mean value in the reference region. ^{18}F-FDOPA PET images consisted of a single six-minute static frame, and parametric images reflecting Standardized Uptake Value Ratios (SUVR) were constructed using the occipital cortex as a reference region. All parametric maps were visually inspected to ensure accurate realignment and reference region normalization.

Parametric images were spatially normalized to a study-specific template in Montreal Neurological Institute (MNI) space using high-dimensional DARTEL registration. PET images were warped using the deformation fields derived from the MRI segmentation (subject-specific gray and white matter tissue class images). We applied an 8 mm full width at half maximum (FWHM) smoothing filter to improve the signal-to-noise ratio. A final voxel size of 2.0 × 2.0 × 2.0 mm^3 was used.

Statistical analysis

The Shapiro-Wilk test was used to check the distribution in all variables. We evaluated the demographical differences between GBA-PD and non-GBA-PD groups using an Welch's test for normally distributed variables and a Mann-Whitney U test, for non-normally distributed data.

To examine the differences in clinical data and their progression over time between the GBA-PD and non-GBA-PD group, a linear mixed-effects model (LMM) was employed using the 'lme4' and 'lmerTest' packages in R. Fixed effects included 'Group' (GBApos vs. GBAneg), 'Time' (since diagnosis), and their interaction (Group × Time), with 'Sex' and 'Age' as covariates. Random intercepts were modelled for each participant (Subject). This analysis was first performed including all participants, and then repeated for the group that had ^{18}F-FDOPA PET. The statistical threshold was set at $p < 0.05$. Statistical analyses were performed using SPSS (version 28.0) and Rstudio (version 2024.9.0.375).

Whole-brain voxel-wise linear mixed effects analyses: Cholinergic and dopaminergic innervation

Whole brain voxel-wise linear mixed effects analyses were conducted using the 3dLME function of Analysis of Functional NeuroImages (AFNI; version 25.1.08)[62–64]. A model with the following Wilkinson notation was fit at each voxel:

$$\text{Y} \sim 1 + \text{Group(GBApos vs.GBAneg)} * \text{Time(since diagnosis)} + \text{Age} + \text{Sex(male vs.female)} + (1|\text{Subject})$$

Time was included as a continuous covariate. F-tests with type III sums of squares were used (by default in 3dLME) to test whether fixed variables (i.e., Group, Time, Group × Time, Age, Sex) explained unique variance.

Results were family-wise error corrected using a threshold of $p < 0.001$ (2-tailed), with a minimum cluster volume of 402 voxels (= 3216 μL) for ^{18}F-FEOBV and 263 voxels (= 2105 μL) for ^{18}F-FDOPA. The latter was determined using Monte Carlo simulation (10,000 iterations) using AFNI's 3dClustSim after estimation of average smoothness across all individuals' smoothed PET images using AFNI's 3dFWHMx (adding the -2difMAD flag)[65]. Post-hoc general linear tests (GLT) were specified in 3dLME to test the direction of effects for categorical fixed variables (i.e., Group and Sex).

To assess the direction of effects within significant clusters for continuous variables, mean PET signal values were extracted for each significant cluster and each participant, and plotted against the continuous variable using the ggplot2 package in R.

To ensure the robustness of our findings, the voxel-wise linear mixed effect analyses were repeated using only de novo PD participants who had both baseline and follow-up PET assessments. The results of these sensitivity analyses are reported in the supplementary material.

Data availability

The data that support the findings of this study are available from the corresponding author, upon reasonable request.

Received: 13 July 2025; Accepted: 16 September 2025;
Published online: 12 November 2025

References

1. Do, J., McKinney, C., Sharma, P. & Sidransky, E. Glucocerebrosidase and its relevance to Parkinson disease. *Mol. Neurodegener.* **14**, 1–16 (2019).
2. Sidransky, E. et al. Multicenter analysis of glucocerebrosidase mutations in Parkinson's disease. *N. Engl. J. Med.* **2009**, 104–105 (2010).
3. Winder-Rhodes, S. E. et al. Glucocerebrosidase mutations influence the natural history of Parkinson's disease in a community-based incident cohort. *Brain* **136**, 392–399 (2013).
4. Brockmann, K. et al. GBA-associated Parkinson's disease: Reduced survival and more rapid progression in a prospective longitudinal study. *Mov. Disord.* **30**, 407–411 (2015).
5. Davis, M. Y. et al. Association of GBA mutations and the E326K polymorphism with motor and cognitive progression in parkinson disease. *JAMA Neurol.* **73**, 1217–1224 (2016).
6. Szwedo, A. A. et al. GBA and APOE impact cognitive decline in Parkinson's disease: a 10-year population-based study. *Mov. Disord.* **37**, 1016–1027 (2022).
7. van der Zee, S. et al. Altered cholinergic innervation in de novo parkinson's disease with and without cognitive impairment. *Movement Disorders* **37**, 1–12 (2022).
8. Okkels, N. et al. Severe cholinergic terminal loss in newly diagnosed dementia with Lewy bodies. *Brain* **146**, 1–15 (2023).
9. Klein, J. C. et al. Neurotransmitter changes in dementia with Lewy bodies and Parkinson disease dementia in vivo. *Neurology* **74**, 885–892 (2010).
10. Bohnen, N. I. et al. Cholinergic system changes of falls and freezing of gait in Parkinson's disease. *Ann. Neurol.* **85**, 538–549 (2019).
11. Pasquini, J., Brooks, D. J. & Pavese, N. The cholinergic brain in Parkinson's Disease. *Mov. Disord. Clin. Pr.* **8**, 1012–1026 (2021).
12. Bohnen, N. I. et al. Cholinergic system changes in Parkinson's disease: emerging therapeutic approaches. *Lancet Neurol.* **21**, 381–392 (2022).
13. Parent, M. et al. PET imaging of cholinergic deficits in rats using [18F] fluoroethoxybenzovesamicol ([18F]FEOBV). *Neuroimage* **62**, 555–561 (2012).
14. van der Zee, S. et al. [18F]Fluoroethoxybenzovesamicol in Parkinson's disease patients: Quantification of a novel cholinergic positron emission tomography tracer. *Mov. Disord.* **34**, 924–926 (2019).
15. Petrou, M. et al. In vivo imaging of human cholinergic nerve terminals with (-)-5- 18F-fluoroethoxybenzovesamicol: Biodistribution, dosimetry, and tracer kinetic analyses. *J. Nucl. Med.* **55**, 396–404 (2014).
16. Slingerland, S. et al. Cholinergic innervation topography in GBA-associated *de novo* Parkinson's disease patients. *Brain* **147**, 900–910 (2024).
17. Filippi, M., Balestrino, R., Basaia, S. & Agosta, F. Neuroimaging in glucocerebrosidase-associated Parkinsonism: a systematic review. *Mov. Disord.* **37**, 1375–1393 (2022).
18. Lopez, G. et al. Longitudinal positron emission tomography of dopamine synthesis in subjects with GBA1 mutations. *Ann. Neurol.* **87**, 652–657 (2020).
19. Liu, G. et al. Specifically neuropathic Gaucher's mutations accelerate cognitive decline in Parkinson's. *Ann. Neurol.* **80**, 674–685 (2016).
20. Bohnen, N. I. et al. Cognitive correlates of cortical cholinergic denervation in Parkinson's disease and parkinsonian dementia. *J. Neurol.* **253**, 242–247 (2006).
21. Shimada, H. et al. Mapping of brain acetylcholinesterase alterations in Lewy body disease by PET. *Neurology* **73**, 273–278 (2009).
22. Bohnen, N. I. et al. Heterogeneity of cholinergic denervation in Parkinson's disease without dementia. *J. Cereb. Blood Flow. Metab.* **32**, 1609–1617 (2012).
23. Goker-Alpan, O. et al. The neurobiology of glucocerebrosidase-associated parkinsonism: A positron emission tomography study of dopamine synthesis and regional cerebral blood flow. *Brain* **135**, 2440–2448 (2012).
24. Barrett, M. J. et al. Transcranial sonography and functional imaging in glucocerebrosidase mutation Parkinson disease. *Parkinsonism Relat. Disord.* **19**, 186–191 (2013).
25. Rinne J. O. et al. Cognitive impairment and the brain dopaminergic system in Parkinson disease: [18F]fluorodopa positron emission tomographic study. *Arch. Neurol.* **57**, 470–475 (2000).
26. Greuel, A. et al. GBA variants in Parkinson's disease: clinical, metabolomic, and multimodal neuroimaging phenotypes. *Mov. Disord.* **35**, 2201–2210 (2020).
27. Caminiti, S. P. et al. Clinical and dopamine transporter imaging trajectories in a cohort of Parkinson's Disease Patients with GBA Mutations. *Mov. Disord.* **37**, 106–118 (2022).
28. Firnau, G. et al. [18F]Fluoro-l-dopa for the in vivo study of intracerebral dopamine. *Int J. Rad. Appl Instrum. A* **37**, 669–675 (1986).
29. Varrone, A. & Halldin, C. Molecular imaging of the dopamine transporter. *J. Nucl. Med.* **51**, 1331–1334 (2010).
30. Lee, C. S. et al. In vivo positron emission tomographic evidence for compensatory changes in presynaptic dopaminergic nerve terminals in Parkinson's disease. *Ann. Neurol.* **47**, 493–503 (2000).
31. Horsager, J. et al. Mapping cholinergic synaptic loss in Parkinson's Disease: An [18F]FEOBV PET case-control study. *J. Parkinsons Dis.* **12**, 2493–2506 (2022).
32. Bohnen, N. I. et al. Cortical cholinergic function is more severely affected in Parkinsonian Dementia Than in Alzheimer disease an in vivo positron emission tomographic study. [date unknown].
33. Gilman, S. et al. Cerebral cortical and subcortical cholinergic deficits in parkinsonian syndromes. *Neurology* **74**, 1416–1423 (2010).
34. Bohnen, N. I. et al. Progression of regional cortical cholinergic denervation in Parkinson's disease. *Brain Commun.* **4**, 1–12 (2022).
35. Gersel Stokholm, M. et al. Cholinergic denervation in patients with idiopathic rapid eye movement sleep behaviour disorder. *Eur. J. Neurol.* **27**, 644–652 (2020).
36. van der Zee, S. et al. Identification of cholinergic centro-cingulate topography as main contributor to cognitive functioning in Parkinson's disease: Results from a data-driven approach. *Front Aging Neurosci.* **14**, 1–12 (2022).
37. van der Zee, S. et al. Cholinergic denervation patterns across cognitive domains in Parkinson's disease. *Mov. Disord.* **36**, 642–650 (2021).
38. Levy, G. et al. Combined effect of age and severity on the risk of dementia in Parkinson's disease. *Ann Neurol*. **51**, 722–729 (2002).
39. Hughes, T. A. et al. A 10-year study of the incidence of and factors predicting dementia in Parkinson's disease. *Neurology* **54**, 1596–1602 (2000).
40. Hu, M. T. M. et al. Predictors of cognitive impairment in an early stage Parkinson's disease cohort. *Mov. Disord.* **29**, 351–359 (2014).
41. Cordes, M. et al. Age-dependent decline of nigrostriatal dopaminergic function: A positron emission tomographic study of grandparents and their grandchildren. *Ann. Neurol.* **36**, 667–670 (1994).
42. Sawle, G. V. et al. Striatal function in normal aging: Implications for Parkinson's disease. *Ann. Neurol.* **28**, 799–804 (1990).
43. Moore, R. Y., Whone, A. L., McGowan, S. & Brooks, D. J. Monoamine neuron innervation of the normal human brain: An 18F-DOPA PET study. *Brain Res.* **982**, 137–145 (2003).
44. Toch, S. R. et al. Physiological Whole-Brain Distribution of [18F] FDOPA uptake index in relation to age and gender: results from a voxel-based semi-quantitative analysis. *Mol. Imaging Biol.* **21**, 549–557 (2019).

45. Aarsland, D. et al. Mild cognitive impairment in Parkinson disease: A multicenter pooled analysis. *Neurology* **75**, 1062–1069 (2010).
46. Kotagal, V. et al. Gender differences in cholinergic and dopaminergic deficits in Parkinson disease. *J. Neural Transm.* **120**, 1421–1424 (2013).
47. Laakso, A. et al. Sex differences in striatal presynaptic dopamine synthesis capacity in healthy subjects. *Biol. Psychiatry* **52**, 759–763 (2002).
48. Kaasinen, V. Ipsilateral deficits of dopaminergic neurotransmission in Parkinson's disease. *Ann. Clin. Transl. Neurol.* **3**, 21–26 (2016).
49. Egerton, A. et al. The test-retest reliability of 18F-DOPA PET in assessing striatal and extrastriatal presynaptic dopaminergic function. *Neuroimage* **50**, 524–531 (2010).
50. Iwaki, H. et al. Genetic risk of Parkinson disease and progression: An analysis of 13 longitudinal cohorts. *Neurol. Genet.* **5** (2019).
51. Boertien, J. M. et al. Study protocol of the DUtch PARkinson Cohort (DUPARC): A prospective, observational study of de novo Parkinson's disease patients for the identification and validation of biomarkers for Parkinson's disease subtypes, progression and pathophysiology. *BMC Neurol.* **20**, 10–11 (2020).
52. d'Angremont, E. et al. Short-latency afferent inhibition as a biomarker of cholinergic degeneration compared to PET imaging in Parkinson's disease [Internet]. *Parkinsonism Relat. Disord.* **121**, 106032 (2024). Available from.
53. Slingerland, S. et al. Cholinergic Degeneration and Cognitive Function in Early GBA1-Related Parkinson's Disease. *Ann Neurol.* https://doi.org/10.1002/ana.27248 (2025).
54. Postuma, R. B. et al. MDS clinical diagnostic criteria for Parkinson's disease [Internet]. *Mov. Disord.* **30**, 1591–1601 (2015). Available from: https://doi.org/10.1002/mds.26424.
55. Schmand, B., Bakker, D., Saan, R. & Louman, J. De Nederlandse Leestest voor Volwassenen: een maat voor het premorbide intelligentieniveau. *Tijdschr. voor gerontologie en. Geriatr.* **22**, 15–19 (1991). Nederlands Instituut voor Gerontologie (NIG). ISSN 0167-9228.
56. den Heijer, J. M. et al. A Large-Scale Full GBA1 Gene Screening in Parkinson's Disease in the Netherlands. *Mov. Disord.* **35**, 1667–1674 (2020).
57. Litvan, I. et al. Diagnostic criteria for mild cognitive impairment in Parkinson's disease: Movement Disorder Society Task Force guidelines. *Mov. Disord.* **27**, 349–356 (2012).
58. Goldman, J. G. et al. Diagnosing PD-MCI by MDS task force criteria: How many and which neuropsychological tests?. *Mov. Disord.* **30**, 402–406 (2015).
59. Emre, M. et al. Clinical diagnostic criteria for dementia associated with Parkinson's disease. *Movement Disorders* **22** (2007).
60. Tomlinson, C. L. et al. Systematic review of levodopa dose equivalency reporting in Parkinson's disease. *Mov. Disord.* **25**, 2649–2653 (2010).
61. Kanel, P. et al. Cerebral topography of vesicular cholinergic transporter changes in neurologically intact adults: A [18F] FEOBV PET study. *Aging Brain* **2**, 100039 (2022).
62. Cox, R. W. & Hyde, J. S. Software tools for analysis and visualization of fMRI data. *NMR Biomed.* **10**, 171–178 (1997).
63. Cox, R. W. AFNI: Software for analysis and visualization of functional magnetic resonance neuroimages. *Computers Biomed. Res.* **29**, 162–173 (1996).
64. Chen, G. et al. Linear mixed-effects modeling approach to FMRI group analysis. *Neuroimage* **73**, 176–190 (2013).
65. Cox, R. W. et al. FMRI Clustering in AFNI: False-Positive Rates Redux. *Brain Connect*. **7** (2017).

Acknowledgements

We thank all patients, caregivers, health-care professionals, and students who have contributed to and collaborated in this project. The inclusion of patients was established with the help of the collaborative Parkinson Platform Northern Netherlands.

Author contributions

S.S. and E.K.R.M. conceptualization; data curation; formal analysis; investigation; methodology; project administration; visualization; writing – original draft H.J.H conceptualization; data curation; formal analysis; investigation; methodology; visualization; writing – original draft S.Z. conceptualization; data curation; formal analysis; funding acquisition; methodology; supervision; writing – review and editing J.M.B. conceptualization; funding acquisition; methodology; supervision; writing – review and editing. G.C. conceptualization; methodology; writing – review and editing S.K.M. conceptualization; methodology; supervision; writing – review and editing I.G. supervision; review and editing E.A. and. A.C.S. Data curation; methodology; project administration; writing – review and editing and T.v.L. conceptualization; funding acquisition; methodology; supervision; writing – review and editing. All authors reviewed the manuscript.

Competing interests

T.v.L. has received grant support from the MJFF, the UMCG, Menzis, Weston Brain Institute and the Dutch Brain Foundation. Consultancy fees were received from AbbVie, Britannia Pharm., Centrapharm and Neuroderm. Speaker fees were received from AbbVie, Britannia Pharm. and Eurocept. J.M.B. has received grant support from the UMCG/RUG, writer fees from Britannia Pharm, speaker fees from Centrapharm, and owns exchange traded funds that might include stocks in medically related fields. The remaining authors declare no competing interests.

Additional information

Supplementary information The online version contains supplementary material available at https://doi.org/10.1038/s41531-025-01160-3.

Correspondence and requests for materials should be addressed to Sofie Slingerland.

Reprints and permissions information is available at http://www.nature.com/reprints

Publisher's note Springer Nature remains neutral with regard to jurisdictional claims in published maps and institutional affiliations.

Open Access This article is licensed under a Creative Commons Attribution-NonCommercial-NoDerivatives 4.0 International License, which permits any non-commercial use, sharing, distribution and reproduction in any medium or format, as long as you give appropriate credit to the original author(s) and the source, provide a link to the Creative Commons licence, and indicate if you modified the licensed material. You do not have permission under this licence to share adapted material derived from this article or parts of it. The images or other third party material in this article are included in the article's Creative Commons licence, unless indicated otherwise in a credit line to the material. If material is not included in the article's Creative Commons licence and your intended use is not permitted by statutory regulation or exceeds the permitted use, you will need to obtain permission directly from the copyright holder. To view a copy of this licence, visit http://creativecommons.org/licenses/by-nc-nd/4.0/.

© The Author(s) 2025